



Eltes, F., Barreto, J., Caimi, D., Karg, S. F., Gentile, A. A., Hart, A., ... Abel, S. (2019). First cryogenic electro-optic switch on silicon with high bandwidth and low power tunability. In *2018 IEEE International Electron Devices Meeting (IEDM)* (Vol. 2018-December, pp. 23.1. 1-23.1. 4). [8614511] (IEEE International Electron Devices Meeting (IEDM)). Institute of Electrical and Electronics Engineers (IEEE).
<https://doi.org/10.1109/IEDM.2018.8614511>

Peer reviewed version

License (if available):
Other

Link to published version (if available):
[10.1109/IEDM.2018.8614511](https://doi.org/10.1109/IEDM.2018.8614511)

[Link to publication record in Explore Bristol Research](#)
PDF-document

This is the accepted author manuscript (AAM). The final published version (version of record) is available online via IEEE at <https://doi.org/10.1109/IEDM.2018.8614511>. Please refer to any applicable terms of use of the publisher.

University of Bristol - Explore Bristol Research

General rights

This document is made available in accordance with publisher policies. Please cite only the published version using the reference above. Full terms of use are available:
<http://www.bristol.ac.uk/pure/about/ebr-terms>

First cryogenic electro-optic switch on silicon with high bandwidth and low power tunability

F. Eltes^{1*}, J. Barreto², D. Caimi¹, S. Karg¹, A. A. Gentile², A. Hart², P. Stark¹, N. Meier¹, M. G. Thompson², J. Fompeyrine¹, S. Abel¹

¹IBM Research – Zurich, Säumerstrasse 4, 8803 Rüschlikon, Switzerland, *email: fee@zurich.ibm.com

²Quantum Engineering Technology Labs, University of Bristol, Bristol, UK

Abstract— We demonstrate the first electro-optic switch operating at cryogenic temperatures of 4 K with a high electro-optic bandwidth of >18 GHz. Our novel technology exploits the Pockels effect in barium titanate thin films co-integrated with silicon photonics and offers low losses, pure phase modulation, and sub-pW electro-optic tuning.

I. INTRODUCTION

To achieve scalable quantum computing, or supercomputers based on rapid single-flux quantum technology, integrated electrical [1, 2] and optical [3, 4] circuits operating at cryogenic temperatures are required. A common challenge among all technologies is the signal interface between the cryogenic processors and the outside world at room temperature (**Fig. 1**) [2]. Currently, the signal transmission relies on electrical wires connecting multiple stages at different temperatures. Here, electrical connections have three major limitations. First, cooling the chip to temperatures at 4 K and below becomes demanding due to the high thermal conductivity of metals and the limited cooling power available. Second, since the bandwidth of single electrical connections is limited, parallel wires would be needed to increase the data throughput, increasing further the total thermal conductivity. Third, increasing the carrier frequency in electrical connections results in larger radio-frequency losses. Such losses are dissipated as heat, which requires a larger fraction of the totally available cooling power.

Fiber-optic connections to transmit signals could solve these issues by providing low power, high-bandwidth data links and low heat-leakage connections at the same time. While some of the building blocks of integrated optical circuits such as light-sources and detectors perform better at cryogenic temperatures, a viable solution for modulators and switches – both key components in optical links – have not yet been found.

Previous demonstrations of integrated electro-optic (EO) switches operated at cryogenic temperatures rely either on thermo-optic phase shifters [5], or on the plasma-dispersion effect, the most common effect in silicon photonic modulators [6]. Both of these approaches suffer from intrinsic limitations: The thermo-optic switches exploit Joule heating to change the refractive index, which requires significant cooling power and which has a low bandwidth of less than MHz [7]. The plasma-dispersion switches rely on very high doping levels in order to compensate for freezing out of charge carriers. Because of the

high doping levels only very small micro-disk resonators can be used in this technology. Tunable low-loss wavelength filters or broadband switches are not feasible due to large insertion losses. In addition, the carrier freeze-out, and therefore a high series resistance, limits the micro-disk resonators to a low bandwidth of <5 GHz at 4.8 K.

The EO Pockels effect does not suffer from the intrinsic limitations of the thermo-optic and plasma-dispersion effects at cryogenic temperatures. However, the Pockels effect requires materials with specific properties, something which has only recently become available in integrated devices compatible with Si photonic platforms and large-scale substrates [8]. Using integrated components based on the Pockels effect it is possible to achieve efficient modulation, low loss, and high bandwidth at cryogenic temperatures. Here, we demonstrate Si photonics-compatible high-speed EO switches based on single-crystal barium titanate (BaTiO₃, BTO) thin-films operating at 4.3 K. We show that losses from BTO are negligible and that static power consumption is minimal. The EO bandwidth exceeds 18 GHz – the highest value achieved to date for an integrated device at cryogenic temperature. Our results prove that integrated BTO-devices are highly suitable for applications in cryogenic photonics (**Fig. 2**).

II. DEVICE STRUCTURE AND FABRICATION

Our electro-optic switches rely on the integration of a thin-film Pockels material in a strip-loaded waveguide geometry (**Fig. 2b**). We use BTO as it is known to have a large Pockels coefficient [9], can be grown on large size Si substrates, and can be integrated in Si photonic platforms [8] (**Fig. 3**). To exclude any electro-optic effects from charge-carriers in a Si waveguide, we employ SiN as the waveguide material. We used an 80-nm-thick BTO layer and a 150-nm-thick SiN layer, structured into a 1.1 μm wide waveguide. This geometry results in 19% mode overlap with BTO for the first order TE mode at 1550 nm (**Fig 2c**). We conservatively designed electrodes separated by 9 μm to ensure the absence of any loss from absorption in the metal. By designing a smaller electrode spacing and improving the electro-optic mode overlap e.g. by thicker BTO layers and different strip-waveguide dimensions, the devices can be optimized for maximal performance. However, the current implementation allows us to evaluate all relevant aspects of BTO as a technology platform for cryogenic EO switches.

We deposited the single-crystal BTO epitaxially on SrTiO₃-buffered 200 nm SOI substrates using a previously reported process [9]. X-ray diffraction shows that we indeed have a high-quality epitaxial BTO layer (Fig. 4). Subsequently, the BTO layer was transferred onto a SiO₂ terminated host wafer via direct wafer bonding, with thin alumina layers serving as bonding interface [10]. The excellent bonding strength yields a transfer ratio close to 100%. After removal of the donor wafer, we deposited 150 nm SiN which was patterned by dry-etching to form the waveguides. We used two-levels of metallization and a 1.5- μ m-thick SiO₂ cladding to add electrodes to the devices (Fig. 5). A high-resolution electron micrograph shows the final cross-section of the BTO/SiN waveguides (Fig. 5f).

III. DEVICE PERFORMANCE

We characterized the electrical and electro-optic properties of our devices in a cryogenic probe station at a temperature of 4.3 K. We measured the electrical and passive optical properties as well as the electro-optic functionality of the devices. By showing broad-band switches, low-power tunable filters, and high-speed modulators, we demonstrate components necessary for a cryogenic photonics platform.

The ferroelectric nature of the BTO film (Fig. 6) can be clearly seen in the electrical current measured between two coplanar electrodes (Fig. 7). The current through our devices at low temperature is extremely low, <500 fA/mm in the operating range. This very small current results in an extremely low static power consumption, which is critical for cryogenic operation. This low leakage current allows us to probe the current generated by ferroelectric domain switching (Fig. 7). Additionally, the electric field dependence of the capacitance also shows the typical hysteretic behavior of ferroelectric materials (Fig. 7) [11].

We extracted propagation losses at 1550 nm of 5.6 \pm 0.3 dB/cm in the waveguides using cut-back measurements performed at room temperature (Fig. 8). In resonant devices we do not observe any increase in losses at 4 K. The propagation losses are only limited by the waveguide fabrication process, as evidenced by identical losses in SiN reference waveguides fabricated with the same process but without any BTO layer (5.4 \pm 0.2 dB/cm). Waveguides with propagation losses <1 dB/cm are available on advanced photonics platforms [12]. Unlike EO switches based on doped Si which suffer high absorption losses, the BTO-photonics technology has no such intrinsic limitation [13].

To demonstrate switching functionality, we employ asymmetric MZMs (Fig. 9) with 500 μ m long phase shifters. Using 2x2 multimode interference splitters we divide the power from the MZM into two outputs (Fig. 10). By applying an electric field to one arm of the MZM we can switch the optical power between the two outputs. In the full range required to switch between the two outputs, the DC power consumption stays below 10 pW (Fig. 11), a record-low number.

Besides low power optical switches, tunable wavelength filters are another important component for quantum optics,

which can be implemented with a tunable resonator (Fig. 12). We use a racetrack resonator with a radius of 50 μ m and 75 μ m long straight phase shifters. We can select the filter wavelength by shifting the resonance position via the electric field bias (Fig. 13). When tracking the resonance position as a function of applied electric field, we see the same hysteretic behavior characteristic of a ferroelectric material as visible in the capacitance measurement (Fig. 14). This hysteresis also enables novel device types and applications in the form non-volatile optical switches [14].

Our technology is capable of high-speed EO modulation at cryogenic temperatures as shown by the S_{21} response of a racetrack modulator. The low Q-factor ($Q \sim 1800$) of the device used for the experiments (Fig. 15) ensures a high intrinsic bandwidth and allows to probe the high-speed EO response of the BTO/SiN phase shifters. We do not reach the 3-dB cut-off of our device within the range of our measurement equipment (18 GHz) (Fig. 16). The high bandwidth in our switches makes the BTO/SiN technology the fastest optical switching technology, to date, for integrated EO devices operating at 4 K (Fig. 17).

IV. CONCLUSION

We have shown the first demonstration of cryogenic operation of integrated EO switches exploiting the Pockels effect. The performance of our devices – low power, low loss, high bandwidth – shows that BTO-based switches can meet all the necessary requirements for optical interconnects in cryogenic systems.

ACKNOWLEDGMENT

This work has received funding from the European Commission under grant agreements no. H2020-ICT-2015-25-688579 (PHRESCO), from the Swiss State Secretariat for Education, Research and Innovation under contract no. 15.0285 and 16.0001, from the Swiss National Foundation project no 200021_159565 PADOMO, from EPSRC grants EP/L024020/1 and EP/K033085/1, the Quantum Technology Capital grant: QuPIC (EP/N015126/1), and ERC grant 2014-STG 640079.

REFERENCES

- [1] J. M. Gambetta *et al.*, *npj Quantum Inf.*, vol. 3, no. 1, p. 2, 2017.
- [2] D. S. Holmes *et al.*, *IEEE Trans. Appl. Supercond.*, vol. 23, no. 3, p. 1701610, 2013.
- [3] J. W. Silverstone *et al.*, *IEEE J. Sel. Top. Quantum Electron.*, vol. 22, no. 6, p. 6700113, 2016.
- [4] J. L. O'Brien *et al.*, *Nat. Photonics*, vol. 3, no. 12, pp. 687–695, 2009.
- [5] A. W. Elshaari *et al.*, *IEEE Photonics J.*, vol. 8, no. 3, 2016.
- [6] M. Gehl *et al.*, *Optica*, vol. 4, no. 3, p. 374, 2017.
- [7] N. C. Harris *et al.*, vol. 22, no. 9, pp. 83–85, 2014.
- [8] F. Eltes *et al.*, in *2017 IEEE International Electron Devices Meeting (IEDM)*, 2017, p. 24.5.1–24.5.4.
- [9] S. Abel *et al.*, *Nat. Commun.*, vol. 4, p. 1671, 2013.
- [10] N. Daix *et al.*, *APL Mater.*, vol. 2, no. 8, p. 086104, 2014.
- [11] D. Bolten *et al.*, *Ferroelectrics*, vol. 221, no. 1, pp. 251–257, 1999.
- [12] P. De Dobbelaere *et al.*, in *2017 IEEE International Electron Devices Meeting (IEDM)*, 2017, p. 34.1.1–34.1.4.
- [13] F. Eltes *et al.*, *ACS Photonics*, vol. 3, no. 9, pp. 1698–1703, 2016.
- [14] S. Abel *et al.*, in *2017 IEEE International Conference on Rebooting Computing (ICRC)*, 2017.

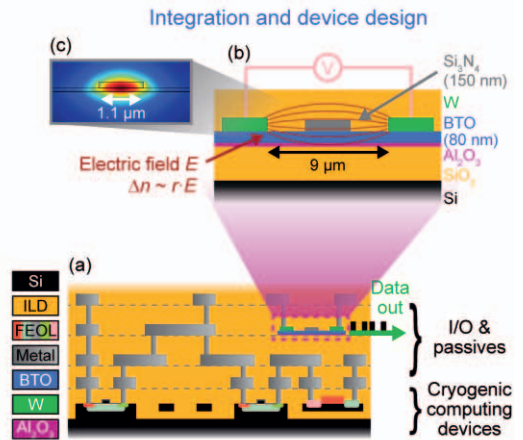
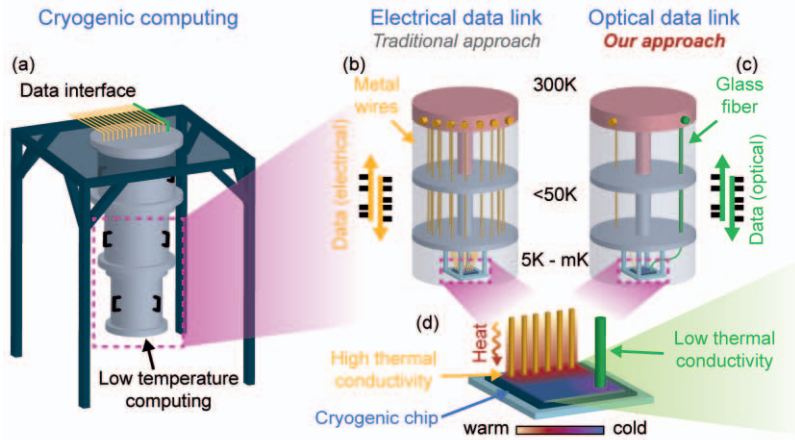


Fig. 1. (a) Schematics of a cryostat typically used for operating cryogenic computing systems. The computing chip is isolated from room temperature via multiple thermal stages with (b) electrical and (c) optical data connections. (d) The high thermal conductivity of multiple electrical connections locally increases the chip temperature and requires more cooling power than thermally insulating, high-bandwidth optical fiber links.

Fig. 2. (a) Integration concept of BTO optical switches in a CMOS compatible process flow as demonstrated in [8]. (b) Cross section of the SiN/BTO optical switch as used in this work. (c) Simulated power distribution of the optical mode in the waveguide center.

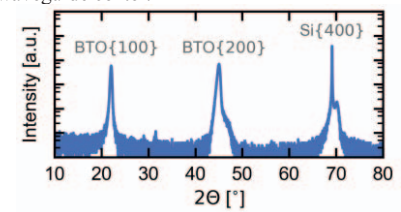
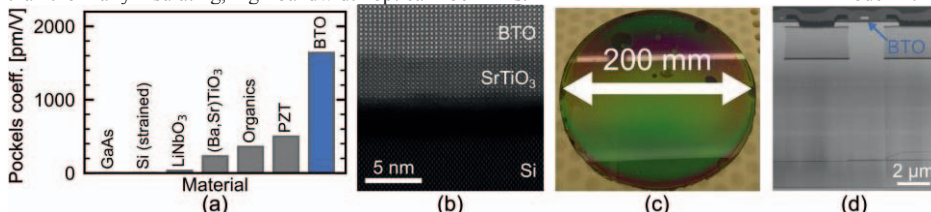


Fig. 3. (a) Comparison of Pockels coefficients in various materials. (b) High-resolution STEM image showing epitaxial BTO film on Si. (c) Demonstration of a wafer bonding transfer of BTO film using 200 mm wafers. (d) Integration of Si-BTO modulators in BEOL of an advanced silicon photonics platform. [8]

Fig. 4. X-ray diffraction spectrum showing good crystal quality, and epitaxial relationship of the BTO on Si used in this work.

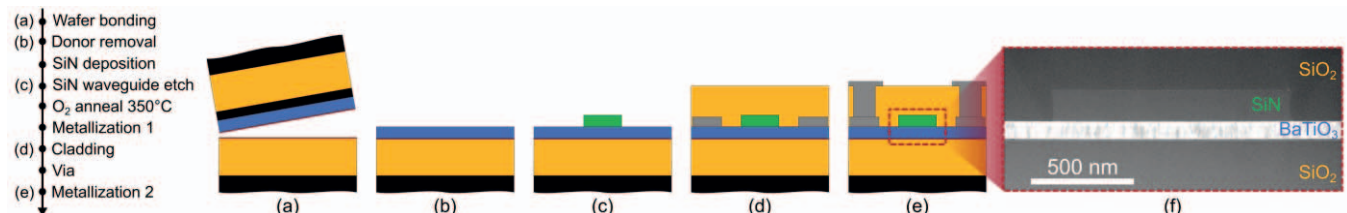


Fig. 5. (a-e) Process flow for fabrication BTO/SiN devices based on single-crystal BTO layers transferred by wafer bonding. (f) STEM image showing the cross-section of a finished BTO/SiN waveguide.

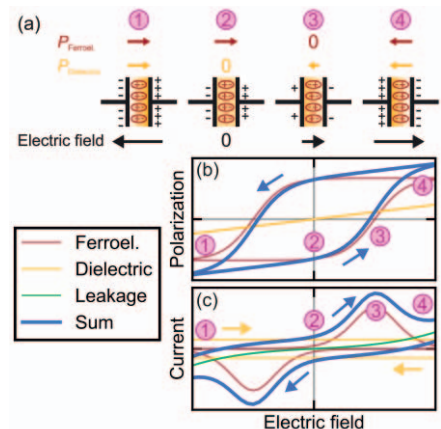


Fig. 6. Change in polarization and resulting electrical current in BTO capacitors. (a) Polarization states in capacitor at different field strengths. The calculated (b) polarization and (c) current show contributions from ferroelectric domain switching, dielectric charging, and leakage.

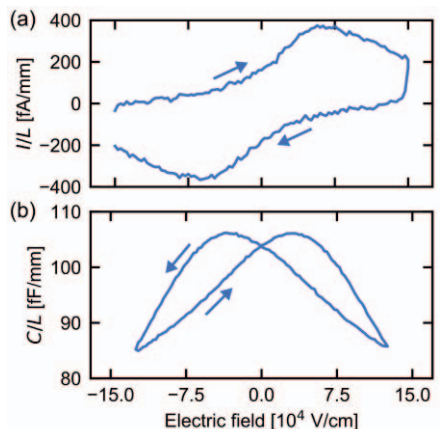


Fig. 7. Normalized (a) current and (b) capacitance across BTO measured at 4.3 K between two electrodes separated by 2 μm. Ferroelectric domain switching and capacitive charging result in the hysteretic behavior (see Fig. 6). The arrows indicate the sweep direction.

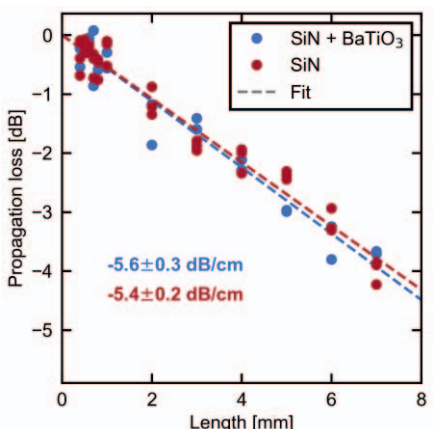


Fig. 8. Propagation losses in the BTO/SiN waveguides, and a reference chip with SiN waveguides fabricated without the bonded BTO layer, both measured at room temperature. The fitted dashed lines correspond to the propagation losses.